The Effect of Global Warming on Severe Thunderstorms in the United States

Jacob T. Seeley and David M. Romps

*Department of Earth and Planetary Science, University of California, Berkeley, and the Earth
Sciences Division, Lawrence Berkeley National Laboratory, Berkeley, California*

ABSTRACT

How will warming temperatures influence thunderstorm severity? This question can be explored by using climate models to diagnose changes in large-scale convective instability (CAPE) and wind shear, conditions that are known to be conducive to the formation of severe thunderstorms. First, an ensemble of climate models from phase 5 of the Coupled Model Intercomparison Project (CMIP5) is evaluated on its ability to reproduce a radiosonde climatology of such storm-favorable conditions in the current climate's spring and summer seasons, focusing on the contiguous United States (CONUS). Of the 11 climate models evaluated, a high-performing subset of four (GFDL CM3, GFDL-ESM2M, MRI-CGCM3, and NorESM1-M) is identified. Second, the twenty-first-century changes in the frequency of environments favorable to severe thunderstorms are calculated in these high-performing models as they are forced by the RCP4.5 and RCP8.5 emissions pathways. For the RCP8.5 scenario, the models predict consistent CONUS-mean fractional springtime increases in the range of 50%–180% by the end of the twenty-first century; for the summer, three of the four models predict increases in the range of 40%–120% and one model predicts a small decrease. This disagreement between the models is traced to divergent projections for future CAPE and boundary layer humidity in the Great Plains. This paper also explores the sensitivity of the results to the relative weight given to wind shear in determining how "favorable" a large-scale environment is for the development of severe thunderstorms, and it is found that this weighting is not the dominant source of uncertainty in projections of future thunderstorm severity.

---

1. Introduction

In the United States, a thunderstorm is classified as "severe" if it produces wind speeds above a damaging threshold, hail exceeding a certain diameter, or a tornado (National Weather Service 2014). These storms down trees, loft roofs, flood roads, ignite fires with their lightning, and damage cars and crops with large hailstones. They are a significant cause of property damage, and are often deadly—in 2011 alone, over 500 people were killed by tornadoes in the United States (NOAA Storm Prediction Center 2012a). In spite of the catastrophic damage caused by severe thunderstorms in the current climate, their response to enhanced greenhouse

forcing remains a poorly understood regional climate change impact (Field 2012; Kunkel et al. 2013).

There are several reasons for this ongoing uncertainty. Most importantly, inconsistent reporting practices have obscured any storm trends that may have accompanied twentieth-century anthropogenic global warming (Brooks and Doswell 2001; Doswell et al. 2005; Verbout et al. 2006; Brooks and Dotzek 2008; Diffenbaugh et al. 2008). As a consequence, research has instead focused on identifying the large-scale "ingredients" of severe convective storms and evaluating how these ingredients will respond to increasing atmospheric greenhouse gas concentrations.

It has been recognized for quite some time that convective available potential energy (CAPE) and deep-layer wind shear—as well as other measures of wind shear, such as helicity—have skill in predicting the severity of thunderstorms in the case that such storms develop at all (Brooks et al. 1994; Rasmussen and Blanchard 1998; Rasmussen 2003). CAPE is a common measure of convective instability and sets an upper bound on the speed of updrafts, while ambient wind shear prolongs and intensifies storms by physically displacing deep-convective

---

Corresponding author address: Jacob Seeley, Department of Earth and Planetary Science, University of California, Berkeley, 449 McCone Hall, Haviland Road, Berkeley, CA 94720.
E-mail: jseeley@berkeley.edu

updrafts from rain shafts and promoting storm-scale rotation. It is not surprising, therefore, that operational weather forecasters use combinations of CAPE and wind shear (along with other information) to issue "watches" for severe thunderstorms, where a watch indicates that meteorological conditions are favorable for the development of severe weather within a few hours (Johns and Doswell 1992). In particular, Brooks et al. (2003) showed that a weighted product of CAPE and 0–6-km wind shear in reanalysis is well correlated with the intensity of nearby observed storms.

The challenge is to determine how CAPE and wind shear—and specifically their regional and subdaily covariation—will change with warming temperatures. Increases in CAPE with global warming have been documented in both climate models (e.g., Sobel and Camargo 2011) and cloud-system-resolving models (Romps 2011), and these increases were recently given theoretical support by Singh and O'Gorman (2013). On the other hand, a first-order prediction for future wind shear calls for a reduced thermal wind gradient, and hence mean shear, as a result of polar amplification of warming (e.g., Trapp et al. 2007a, hereafter T07). These qualitative predictions for how global warming should affect CAPE and wind shear have opposing implications for the severity of future thunderstorms.

In light of this opposition, several recent climate model studies have attempted to quantitatively settle the competition between increasing CAPE and decreasing shear. T07 performed the first multimodel comparison of future severe thunderstorms in the United States and found significant divergence between a regional climate model and three general circulation models (e.g., their Fig. 3). Trapp et al. (2009) used NCAR's CCSM3 to predict increases in CAPE that outpaced decreases in wind shear, resulting in an increase in environments favorable for severe thunderstorms; however, results from a single GCM should not be given too much weight, considering the disagreement between models shown in T07. Most recently, Diffenbaugh et al. (2013, hereafter D13) expanded on the results of T07 with an enlarged ensemble of 10 GCMs from the archive of phase 5 of the Coupled Model Intercomparison Project (CMIP5) (Taylor et al. 2012). D13 found robust increases in the frequency of severe-thunderstorm environments in the spring and fall across most of the United States, again as a result of increases in CAPE that were large enough to overcome decreases in wind shear. However, the ensemble of models used in D13 diverged significantly in its predictions for the summer months of June–August (JJA), which constitute half of the peak severe-thunderstorm season in the current climate (Kelly et al. 1985). The lingering uncertainty

regarding these important months merits additional study.

Furthermore, in the context of these studies, it is clear that the relative weight given to CAPE and shear in defining storm-favorable conditions is of central importance; depending on this weighting, the same fractional changes in CAPE and shear derived from a climate model's global warming response could lead to quite different conclusions about changes in the frequency of severe thunderstorms. In fact, multiple studies have argued that the value of ambient wind shear is more strongly tied to a given thunderstorm's severity than the background CAPE (Brooks et al. 2003; Allen et al. 2011; Brooks 2013). However, previous climate model studies of the effect of global warming on severe thunderstorms in the United States have used a threshold for the unweighted product of CAPE and shear to define when a GCM grid point is favorable for storms. This discrepancy between observational severe-thunderstorm proxies and the proxies that have been used in previous modeling studies is an unnecessary source of uncertainty in our current understanding of the future of thunderstorms.

The present study puts this line of research on more solid ground in two major ways. First, since the ensemble of climate models in D13 was not selected based on demonstrated skill at replicating the contemporary climatology of severe-thunderstorm conditions, it is plausible that some of the divergence in their ensemble's predictions for the future, especially in the summer, can be traced to differences between the models in their base state of simulated severe-thunderstorm conditions. To test this hypothesis, in section 2, we derive an observational climatology of United States severe-thunderstorm environments from a decade of radiosonde observations and evaluate an ensemble of 11 CMIP5 climate models on its ability to capture the spatial pattern of these observations throughout the principal severe-thunderstorm season of March–August. Second, in section 3, we focus on the changes in severe-thunderstorm conditions predicted by the high-performing subset of models identified in section 2 as they respond to the range of greenhouse forcing spanned by the RCP4.5 and RCP8.5 emissions scenarios (van Vuuren et al. 2011). We explore the sensitivity of our results to the relative weight given to CAPE and shear in the definition of a severe-thunderstorm environment by repeating our analysis of future changes for a plausible range of shear weightings. Some conclusions and directions for future work are presented in section 4.

2. Evaluating the GCMs

The predictions of a global climate model (GCM) about the future of severe thunderstorms are more trustworthy

TABLE 1. The GCMs included in this study. Resolution is indicated in terms of (lon points) × (lat points) × (levels in the vertical). Expansion of GCM acronyms is available online at http://www.ametsoc.org/PubsAcronymList.

GCM	Institute	Resolution
BCC_CSM1.1	Beijing Climate Center	$128 \times 64 \times 26$
BCC_CSM1.1(m)	Beijing Climate Center	$320 \times 160 \times 26$
CanESM2	Canadian Centre for Climate Modelling and Analysis	$128 \times 64 \times 35$
CCSM4	National Center for Atmospheric Research	$288 \times 192 \times 26$
CNRM-CM5	Centre National de Recherches Météorologiques	$256 \times 128 \times 31$
FGOALS-g2	Institute of Atmospheric Physics, Tsinghua University	$128 \times 60 \times 26$
GFDL CM3	Geophysical Fluid Dynamics Laboratory	$144 \times 90 \times 48$
GFDL-ESM2M	Geophysical Fluid Dynamics Laboratory	$144 \times 90 \times 24$
MIROC5	Japan Agency for Marine-Earth Science and Technology	$256 \times 128 \times 40$
MRI-CGCM3	Meteorological Research Institute	$320 \times 160 \times 48$
NorESM1-M	Norwegian Climate Centre	$144 \times 96 \times 26$

if the model demonstrates skill at simulating where and how frequently these storms occur in the current climate. Unfortunately, since the typical size of thunderstorms (~25 km in diameter) remains below the threshold of resolution for current-climate models, evaluating models requires identifying severe-thunderstorm-favorable environments (STEnvs) when the large-scale conditions of CAPE and wind shear are simultaneously abundant at the scale of a GCM grid cell. A loose analogy can be drawn between STEnvs and the severe-thunderstorm watches issued for the United States by the National Weather Service's Storm Prediction Center, although the latter typically cover an area larger than a GCM grid cell and are issued by meteorologists with access to more detailed characterizations of the atmosphere (Johns and Doswell 1992). Clearly the application of such individual expertise is not feasible for the systematic analysis of large quantities of GCM data. Nevertheless, the framework of severe-thunderstorm watches is instructive in the context of GCMs that do not resolve thunderstorms because a "watch" indicates only that atmospheric conditions are primed for the development of a storm, not that one has yet been observed. (This is in contrast to "warnings," which are issued once a storm has been confirmed.) Identifying storm-favorable environments based on the ambient levels of CAPE and wind shear in the weather of a climate model results in a picture of where and when the simulated atmosphere could have supported severe thunderstorms.

To benchmark GCMs against observations of severe-thunderstorm conditions, we have derived maps of CAPE and 0–6-km wind shear at 1° resolution over the continental United States (CONUS) at 0000 UTC—from mid- to late afternoon local time, the peak hours of severe-thunderstorm formation (Kelly et al. 1985)—from a decade of radiosonde data as well as CMIP5 output for each of 11 GCMs. The radiosonde observations are provided by the Stratosphere–Troposphere

Processes and their Role in Climate (SPARC; World Climate Research Programme 2014) high-vertical-resolution radiosonde data (HVRRD); each 0000 UTC sounding is filtered to detect instrument malfunction and interpolated to a uniform 100-m vertical resolution. The 11 CMIP5 GCMs we evaluate, listed in Table 1, have a range of spatial resolutions and are drawn from modeling agencies from around the world (Taylor et al. 2012). CAPE was calculated assuming the adiabatic, undiluted ascent of a near-surface parcel of air; parcel densities were computed using a root solver and an exact expression for equivalent potential temperature derived by Romps and Kuang (2010), which includes the effects of latent heat of fusion and the different heat capacities of the water phases. Wind shear was calculated as the magnitude of the vector difference between the near-surface winds and the winds at a pressure level with a mean altitude of 6 km above the ground. For more details about the radiosonde network, the ensemble of GCMs, and the calculation of CAPE and wind shear, see the appendix.

Throughout this work, we identify 1° cells in the continental United States as STEnvs whenever the weighted product of CAPE ($J kg^{-1}$) and shear ($m s^{-1}$) in that cell at 0000 UTC exceeds a threshold. The criterion for STEnvs can be generally expressed as

$$(\text{CAPE})(\text{shear})^{\gamma} \geq \beta, \tag{1}$$

where γ is the relative weight given to shear and β is a threshold value $[(m s^{-1})^{2+\gamma}]$. There are numerous precedents for using such a discriminator line in CAPE–shear phase space to identify large-scale environments that are conducive to the formation of severe thunderstorms. Brooks et al. (2003) found that Eq. (1) with $\gamma = 1.6$ and $\beta = 46\,800$ $(m s^{-1})^{3.6}$ was most effective at detecting reanalysis "pseudo soundings" associated with significant severe thunderstorms in the United States,
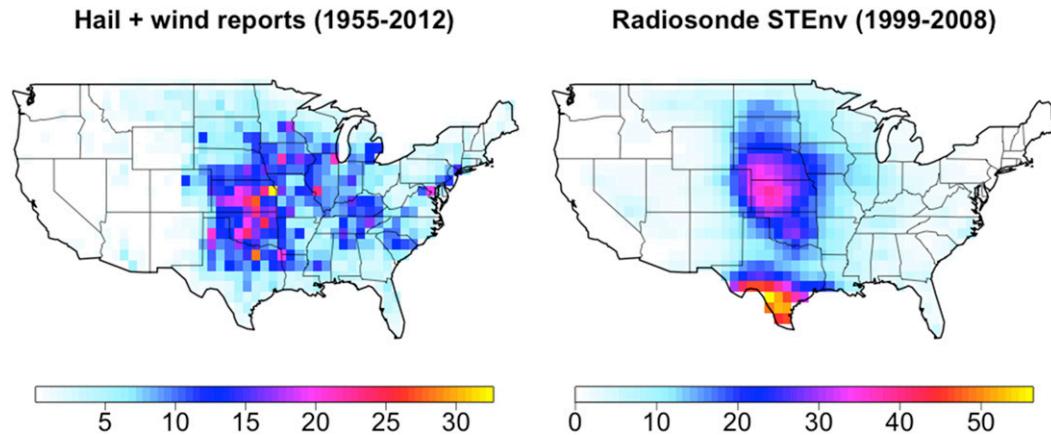
Hail + wind reports (1955-2012)   **Radiosonde STEnv (1999-2008)**

FIG. 1. (left) Mean annual reports $[(°)^{-2}]$ of hail greater than 1 in. in diameter or winds in excess of 50 knots [kt $(1\,\text{kt} = 0.51\,\text{m s}^{-1})$], from 1955 to 2012 (NOAA Storm Prediction Center 2012b). Reports are binned in 1° cells based on the latitude and longitude coordinates recorded for the report by the Storm Prediction Center. (right) Mean annual STEnvs [days per year with (CAPE)(shear) $\geq 36\,300\,(\text{m s}^{-1})^3$ at 0000 UTC] derived from the SPARC radiosonde network for the years 1999–2008.

while Allen et al. (2011) found that $\gamma = 1.67$ and $\beta = 115\,000\,(\text{m s}^{-1})^{3.67}$ could do the same for short-term forecasts from a numerical weather prediction model for Australia. Both of these studies used databases of observed thunderstorms and arrived at $\gamma > 1$, reflecting that the value of environmental shear is apparently of greater importance than the local CAPE in determining the severity of a given thunderstorm. Building on these insights, Allen et al. (2014a,b) used a discriminator line with $\gamma = 1.67$ in a detailed study of current and future severe-thunderstorm environments in Australia. On the other hand, climate model studies of severe-thunderstorm environments in the United States have almost exclusively used $\gamma = 1$ and $\beta = 10\,000\,(\text{m s}^{-1})^3$ (Marsh et al. 2007; T07; Trapp et al. 2009; D13), with one study using $\beta = 20\,000\,(\text{m s}^{-1})^3$ (Gensini et al. 2014). One purpose of the present study is to quantify the extent to which previous work may have reported inflated increases in United States severe-thunderstorm environments as a result of underweighting the effect of future decreases in shear.

However, for the purpose of evaluating climate models on their simulation of current-climate severe-thunderstorm conditions, we take $\gamma = 1$ and $\beta = 36\,300\,(\text{m s}^{-1})^3$. The choice of $\gamma = 1$ in this section was made for simplicity and in order to have the most contact with previous multimodel studies of United States severe thunderstorms; in any case, the value of γ is much more important when considering trends in STEnvs than it is when seeking a general picture of GCM performance in the current climate, and γ will be allowed to vary substantially in section 3 when we analyze trends in STEnvs. The chosen value of β selects the upper 3% of

(CAPE)(shear) in the radiosonde data, and was found to result in a mean annual number of STEnvs that compares well with what was found in reanalysis by D13 and others, building confidence that we are considering a similarly extreme population of CAPE and shear combinations despite potential differences in the calculation of CAPE.

NOAA climatologies of past severe-thunderstorm watches indicate that the region of peak storm activity in today's climate is the central United States, beginning east of the Rocky Mountains, extending from the middle of Texas north to the Dakotas, and tailing off toward the East Coast (NOAA Storm Prediction Center 2012b). This region of significant severe-thunderstorm activity in the central United States is readily apparent in historical reports of large hail and severe convective winds (Fig. 1, left), and is the most salient feature of the current climate's pattern of severe-thunderstorm activity. Overall, Fig. 1 shows that the climatology of STEnvs derived from radiosondes is well correlated with the region of observed severe-thunderstorm damage in the central United States.

An exception is the region of southern Texas, where a large number of STEnvs occur but there have been few reports of severe-thunderstorm damage. This feature has been noted previously in United States reanalysis by Gensini and Ashley (2011) and others, and highlights an important point about what information can be gleaned from STEnvs. STEnvs do not account for factors that are known to be closely tied to storm initiation—from small-scale outflow boundaries to large-scale inversions—and are therefore agnostic about whether thunderstorms actually occurred. It is well known that southern Texas is frequently capped by an elevated mixed layer that is

advected eastward from the high desert terrain of the Mexican Plateau (Carlson and Ludlam 1968). In the absence of mechanisms to erode the inversion, this "lid" has such a strong inhibiting effect on thunderstorm formation in southern Texas that, even though CAPE and shear are abundant, severe thunderstorms are rare.

Clearly, this uncertainty regarding storm initiation limits our ability to translate trends in STEnvs into projections for future severe thunderstorms. Changes in the processes that inhibit and promote storm initiation, which cannot at present be resolved by GCMs, may have an attenuating or amplifying effect on the way STEnv trends will influence future thunderstorms. Van Klooster and Roebber (2009) derived an index of convective initiation potential from the large-scale variables resolved by climate models and found no change in this initiation potential over the twenty-first century, but that study only considered a single GCM. Another promising avenue for studying convective initiation is dynamically downscaling GCM output with a high-resolution regional climate model that can explicitly resolve convective storms, although such results are still model dependent and generating long integrations with this technique is computationally intensive (Trapp et al. 2007b, 2011; Robinson et al. 2013). A self-contained multimodel analysis of future changes in convective initiation may become a tractable problem only once GCM resolutions have substantially improved. Therefore, for the moment the best one can do is assume that the fraction of STEnvs that develop severe storms will be the same in the future as in the present, but there is not much to justify this assumption besides necessity.

With these limitations in mind, it is encouraging that the observational climatology of STEnvs does highlight the region of maximum severe-thunderstorm damage in the central United States. It is also worth noting the similarity between the radiosonde observations in Fig. 1 (right) and the distribution of severe-thunderstorm environments found previously in reanalysis by, for example, Brooks et al. (2003) and D13. Given the widely recognized deficiencies in the ability of reanalysis fields to represent sharp vertical gradients of thermodynamic quantities (Gensini et al. 2014), it was not a foregone conclusion that severe-thunderstorm conditions estimated from high-vertical-resolution radiosonde data would not appear substantially different from those derived from reanalysis. The similarity of the radiosonde climatology of STEnvs presented here with reanalysis data confirms that reanalysis is a suitable tool for the study of large-scale environments associated with severe thunderstorms.

But how well can CMIP5 GCMs reproduce the observed pattern of storm activity? About 93% of STEnvs

in the radiosonde data occur between the months of March and August, and it has been previously noted by Kelly et al. (1985) that more than 80% of thunderstorms producing damaging winds and large hail occur during these months. Therefore, we focus our analysis on the spring [March–May (MAM)] and summer (JJA) seasons. Figures 2a–l and 3a–l show the climatologies of STEnvs derived from the radiosonde data and 11 CMIP5 climate models for the current climate's spring and summer seasons, respectively. The differences in model skill are most apparent during summer, when there is significant spread in how well the climate models capture the radiosonde observations' concentration of STEnvs in the central United States. A majority of the GCMs depicted in Fig. 3 predict that much of the East Coast of the United States should be at least as frequently favorable for the development of summertime severe thunderstorms as the Great Plains, in stark contrast to the radiosonde observations, and some models actually have local STEnv minima in the Great Plains [e.g., BCC_CSM1.1(m) and CanESM2]. These differences between the models are not nearly as apparent for the spring months shown in Fig. 2, when most models qualitatively capture the concentration of STEnvs creeping up from Texas into the southern Great Plains. A likely explanation for the better performance of the models in the spring is the predominance of synoptic forcing, which is on a scale better resolved by GCMs, as compared to the mesoscale-system-dominated summer (Fritsch et al. 1986).

The GCM ensemble's performance is summarized in Figs. 2m and 3m, where we show pattern correlations between the climatologies of STEnvs for the radiosonde data and the GCMs. We also quantify the overall seasonal bias in the number of STEnvs that occur in the GCMs. The pattern correlations confirm that many of the GCMs in our ensemble have very little predictive power in the summer. In this work, we stipulate that a GCM must have a pattern correlation of 0.5 for both MAM and JJA current-climate STEnvs (R^2 in Figs. 2m and 3m) in order to be considered skillful at simulating severe-thunderstorm conditions. According to this criterion, the four high-performing models are GFDL CM3, GFDL-ESM2M, MRI-CGCM3, and NorESM1-M. The principal difference between high- and low-performing GCMs is the zonal distribution of STEnvs in the summer: the high-performing group has its summertime peak of STEnvs in the central United States, collocated with the defining feature of the radiosonde observations. On the other hand, the low-performing GCMs display a much broader swath of STEnvs and/or significant peaks in activity on the East Coast in the summer. When we consider the effect of global warming on STEnvs in
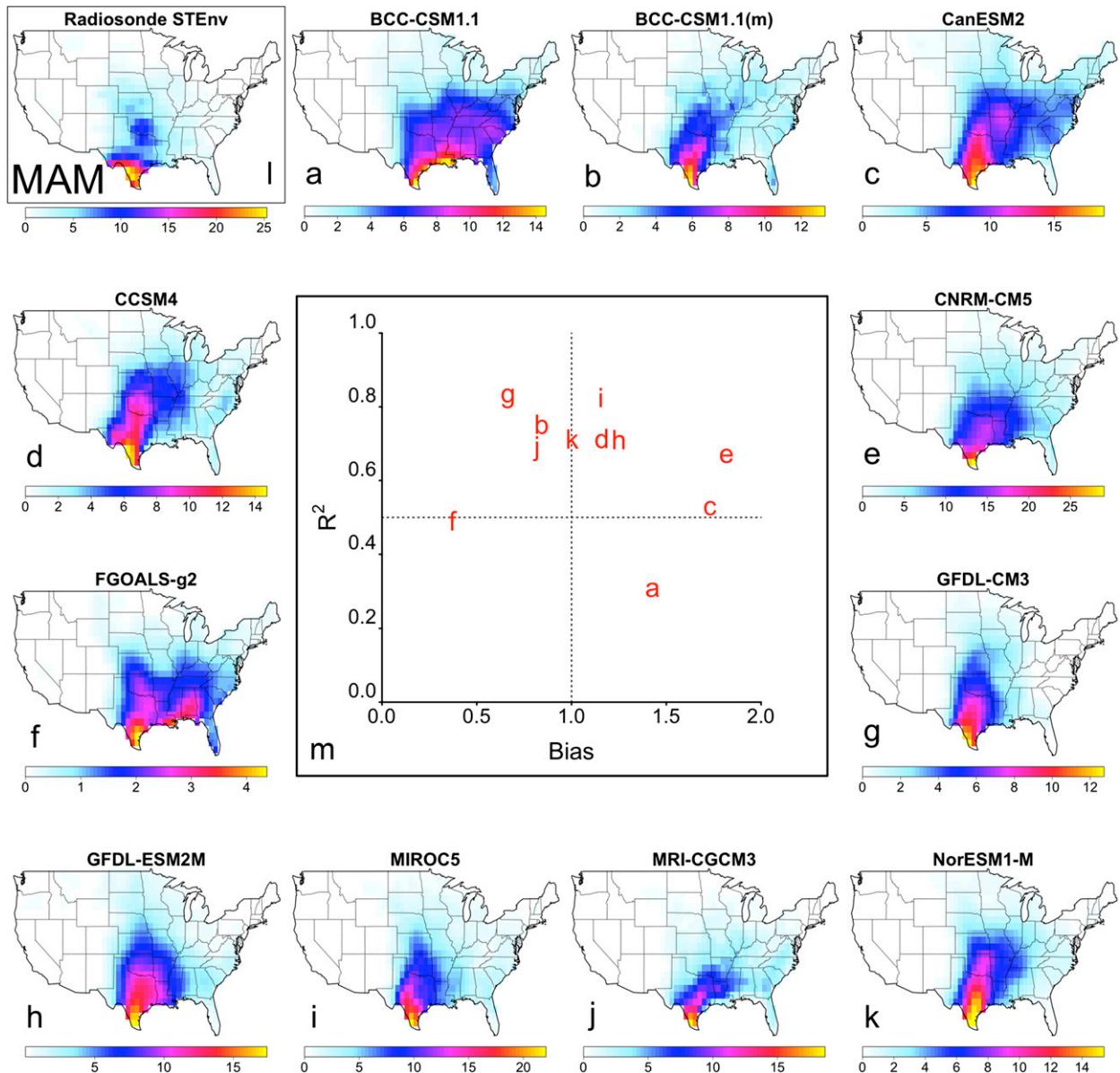
FIG. 2. Mean STEnvs per MAM for (a)–(k) the years 1996–2005 in 11 CMIP5 GCMs and (l) the years 1999–2008 in SPARC radiosonde observations. (m) A summary of the ability of the 11 GCMs in our ensemble to simulate the radiosonde observations. The ordinate of (m) is the spatial coefficient of determination R^2 and is a measure of how well a GCM's geographical distribution of STEnvs matches the distribution in the radiosonde data. The abscissa ("Bias") is the ratio of a GCM's CONUS-mean STEnvs (land grid points only) to that of the radiosonde climatology, and thus is a measure of how well a GCM predicts the observed number of STEnvs per season per year.

section 3, we will focus our attention on this subset of high-performing models to see if they display a more consistent summertime response than was found for the larger ensemble of D13. However, given the inherent subjectivity in evaluating climate models to determine which are "high performing" (Tebaldi and Knutti 2007), we will also present a summary of results for all 11 GCMs in our ensemble.

3. Severe thunderstorms in a warm future United States

The high-performing models identified in section 2 are used here to predict changes in thunderstorm severity approximately 75 years in the future. We use CMIP5 data from the decade 2079–88 of the RCP4.5 and RCP8.5 experiments to represent the future climate under medium
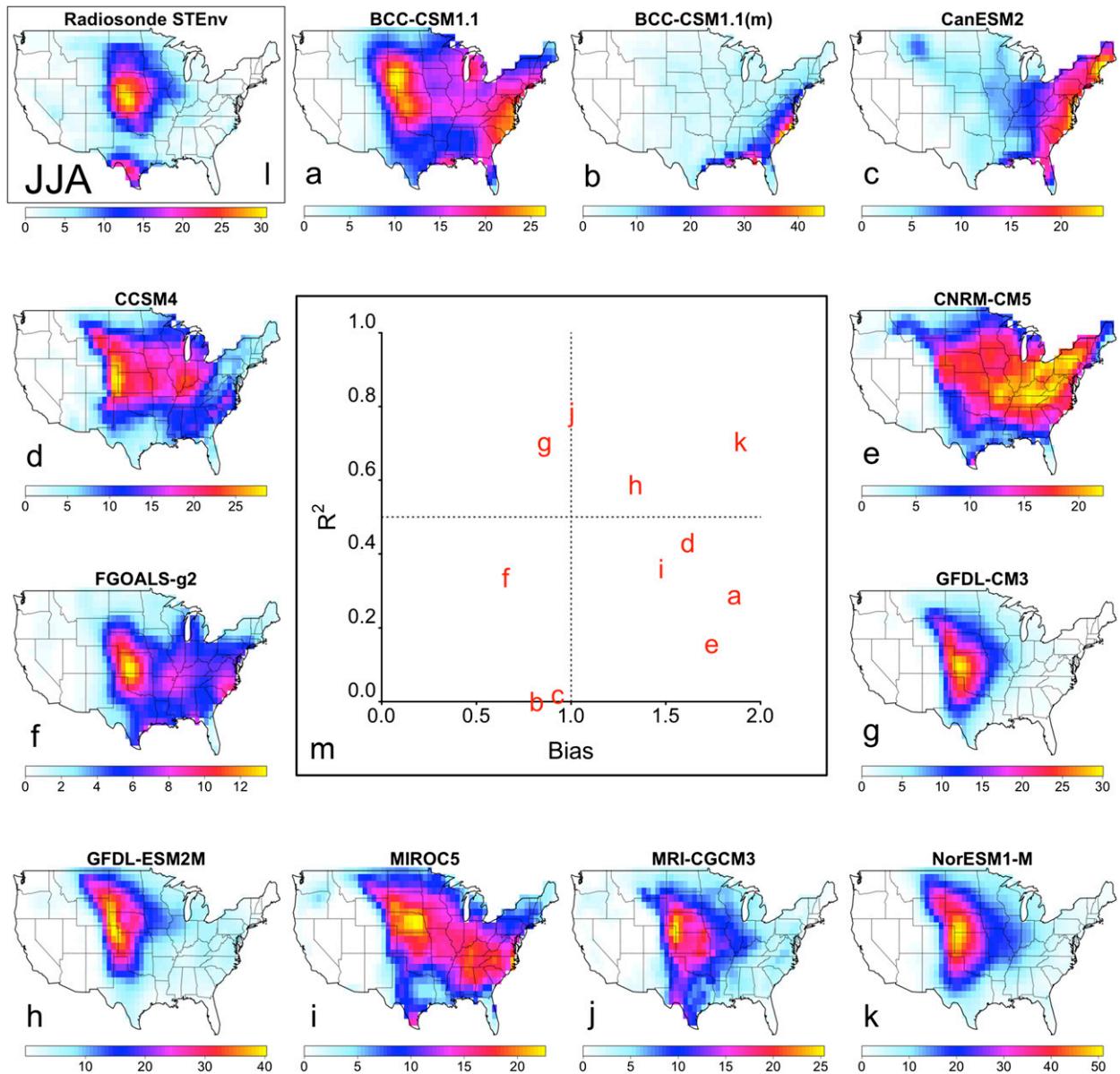
FIG. 3. As in Fig. 2, but for JJA.

and high levels of greenhouse forcing, respectively (van Vuuren et al. 2011), and identify STEnvs in the simulated weather of the GCMs for this decade using the same method presented in section 1. Under the assumption that the same fraction of STEnvs will be actualized into storms in the future as at present, changes in STEnvs tell us about how GCMs predict the frequency of severe thunderstorms will change. In section 3a, we again use $\gamma = 1$ and $\beta = 36\,300\,(\mathrm{m\,s}^{-1})^3$ as a (CAPE)(shear)$^\gamma$ threshold, allowing us to diagnose how often in each GCM's simulated future the subdaily product of CAPE and shear at local mid- to late afternoon would cause the environment to be classified as

a STEnv. The sensitivity of changes in STEnvs to the relative weight given to shear is explored in section 3b.

a. $\gamma = 1$ (CAPE and shear equally weighted)

The changes in annual-mean spring and summer STEnvs due to global warming are shown for the high-performing GCMs in Figs. 4 and 5, respectively. To probe the models' response to a range of radiative forcing, we show results for both the RCP4.5 and RCP8.5 greenhouse emissions scenarios, which respectively represent medium-mitigation and high-carbon business-as-usual pathways (van Vuuren et al. 2011). Figure 4 shows that
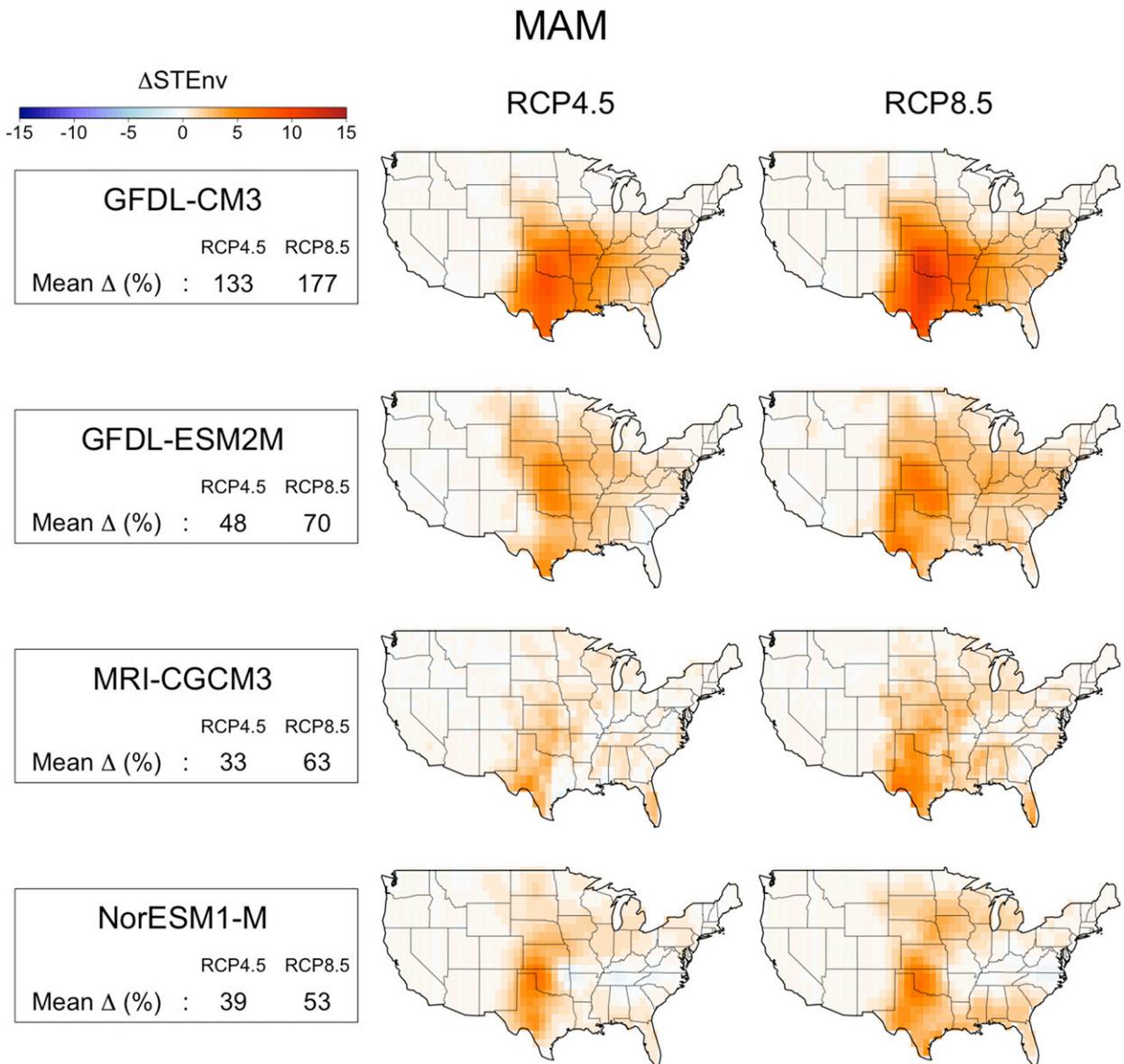
FIG. 4. Changes due to global warming in annual-mean STEnvs during MAM in the high-performing GFDL CM3, GFDL-ESM2M, MRI-CGCM3, and NorESM1-M. Results for both the RCP4.5 and RCP8.5 greenhouse gas forcing scenarios are presented. Changes are calculated as the mean of the period 1996–2005 of the CMIP5 historical experiment subtracted from the mean of the period 2079–88 of the RCP experiment. A summary of the fractional CONUS-mean changes is given for each of the four models in the boxes at left.

in the spring, the ensemble of high-performing models predict a consistent response of increased STEnvs extending from Texas into the southern and central Great Plains. This region of increase coincides with the current climate's spatial pattern of STEnvs—evident in both the radiosonde and GCM data shown in Fig. 2—suggesting a "stormy gets stormier" response for springtime severe thunderstorms. These results agree with those of D13, who found consistent increases in severe-thunderstorm environments during the spring for a 10-member ensemble of

CMIP5 models. The trends for this season are robust to the range of greenhouse forcing spanned by the RCP4.5 and RCP8.5 scenarios, with the magnitude of predicted CONUS-mean increases ranging from 30% to 150% for the RCP4.5 scenario, and from 50% to 180% for the RCP8.5 scenario. The fact that the increases for the RCP4.5 scenario are smaller than the RCP8.5 increases by 20%–50% suggests that the climate policies adopted in the coming decades will affect the severity of the spring thunderstorm season in the United States.
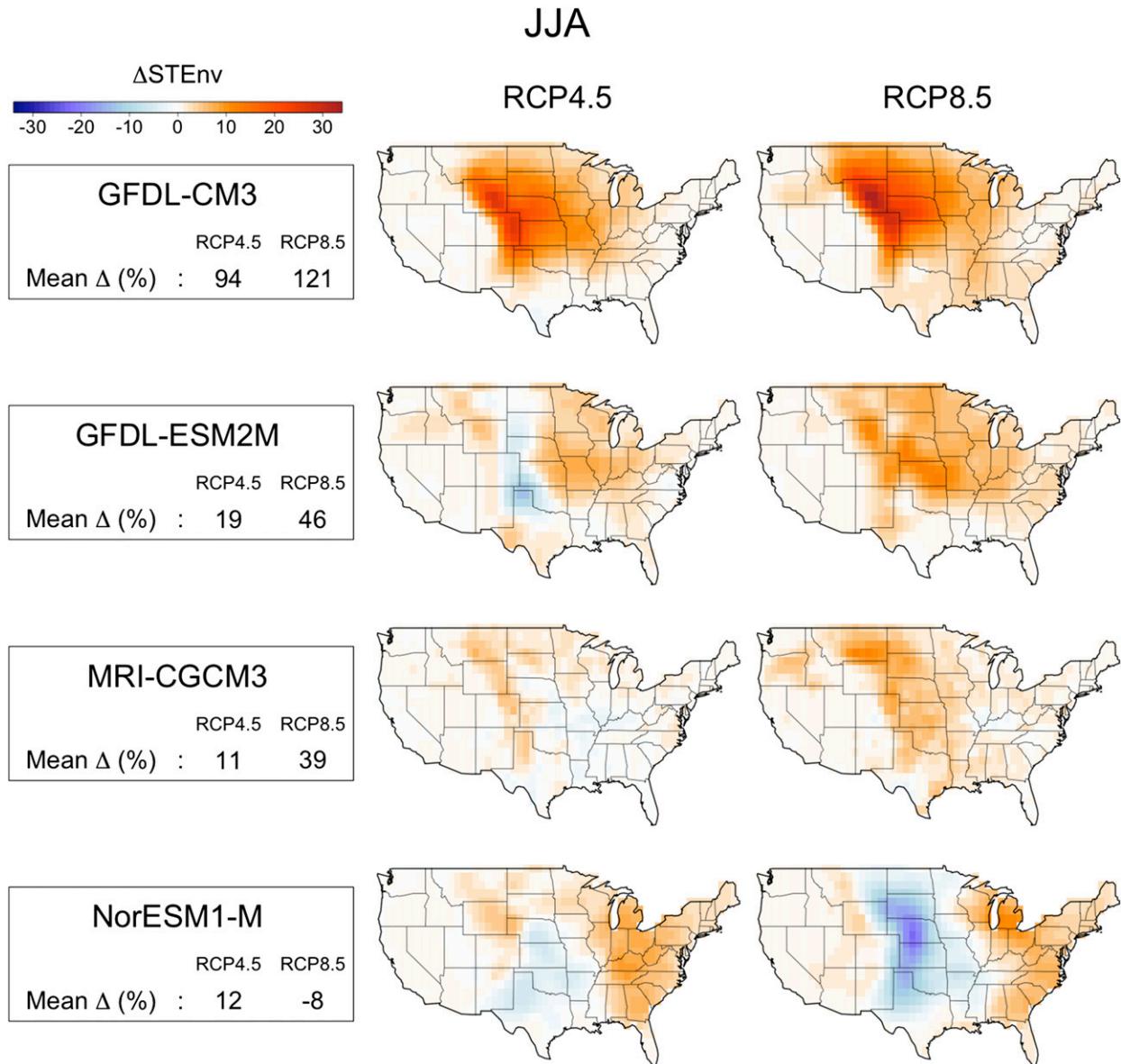
JJA

FIG. 5. As in Fig. 4, but for JJA.

The summertime response of the high-performing ensemble of models is considerably more diverse (Fig. 5). For the RCP8.5 scenario, three of the four high-performing models predict increases in the range of 40%–120%, while one model (NorESM1-M) predicts an approximately 10% decrease. In all cases, these changes are concentrated in the central and northern Great Plains, around the climatological maximum of STEnvs for the current-climate radiosonde data and four high-performing GCMs shown in Fig. 3. In contrast to the spring season, during the summer the RCP4.5 response is qualitatively different from the RCP8.5 response for two of the models, changing sign locally in the central

Great Plains for GFDL-ESM2M and in the CONUS mean for NorESM1-M.

One source of motivation for the present study was the hypothesis that a restricted ensemble of CMIP5 climate models, selected for its demonstrated skill at matching a radiosonde climatology of STEnvs, might display a more consistent response to greenhouse forcing than the larger ensemble used by D13, particularly in the summer. The results shown in Fig. 5 partially discredit this hypothesis, because the four highest-performing models identified in section 2 do not agree on even the sign of CONUS-mean changes in the frequency of summer STEnvs under the strong radiative
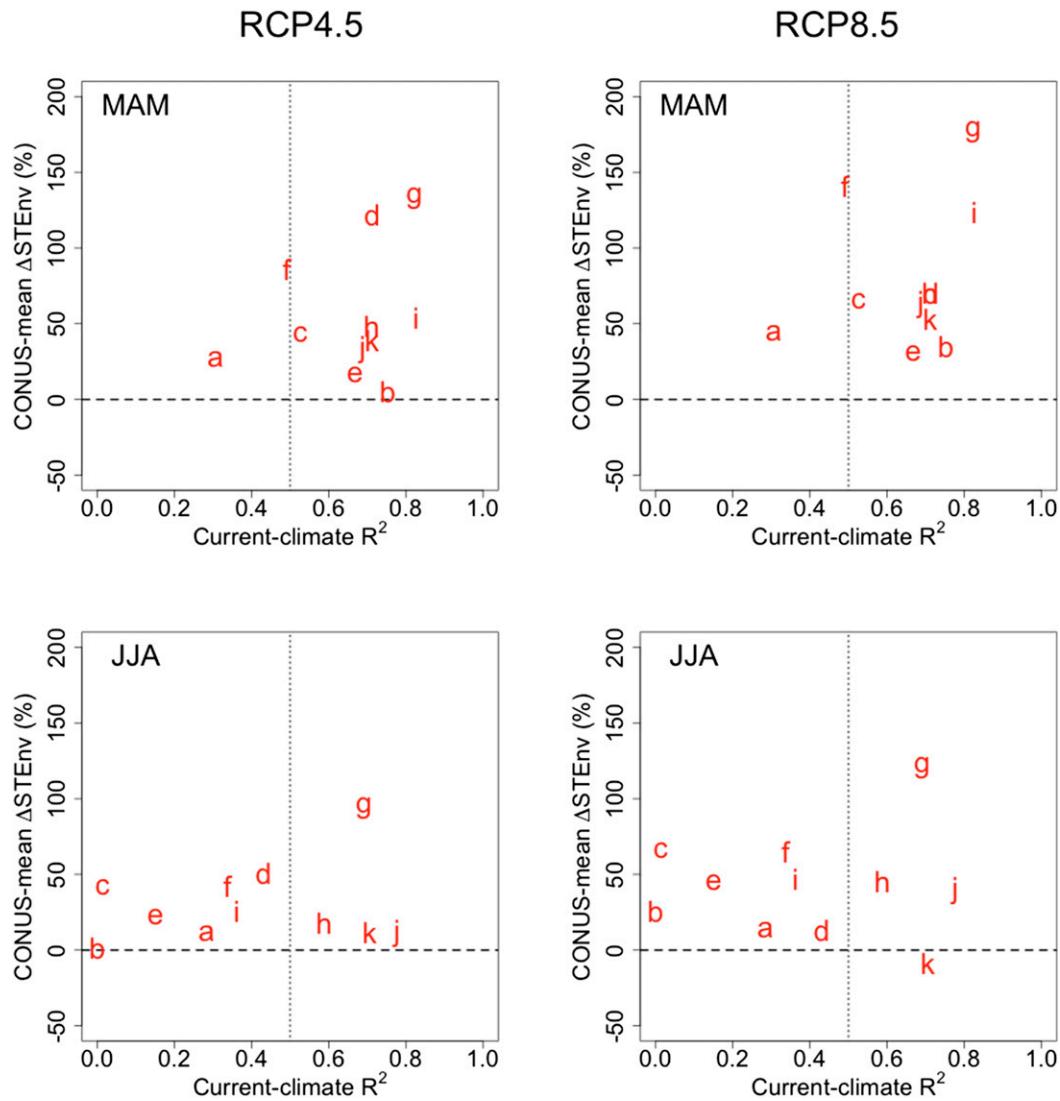
FIG. 6. Changes in MAM and JJA CONUS-mean STEnvs in the 11 GCMs listed in Table 1, as a function of their R^2 "score" on their ability to match the spatial pattern of observed current-climate STEnvs. The letters a–k correspond to the same models as in Figs. 2 and 3; the "high performing" models are those that have an R^2 above 0.5 for both MAM and JJA.

forcing of the RCP8.5 scenario, and there is no clear distinction between the response of the "high performing" and "low performing" models in CONUS-mean percent increases in STEnvs (Fig. 6).

However, there is a clear outlier among the high-performing models: NorESM1-M predicts decreases in summer STEnvs throughout the Great Plains—unlike GFDL CM3, GFDL-ESM2M, and MRI-CGCM3, which together show a consistent increase in this region when forced by RCP8.5-level emissions. Variations in simulated future shear are not the source of the difference between NorESM1-M and the other three models, as all four of these models predict decreasing

CONUS-wide wind shear in the range from −5% to −14% for this season under RCP8.5 forcing. However, NorESM1-M is a significant outlier in this small ensemble of high-performing models for its predicted changes in CAPE and boundary layer humidity (Fig. 7). While the GFDL models and MRI-CGCM3 predict increases in CAPE on the order of 1 kJ kg^{-1} throughout the Great Plains, NorESM1-M predicts that mean summertime CAPE will decrease by roughly 500 J kg^{-1} in this region. The increases in CAPE in the first three models appear to be driven by increases in boundary layer specific humidity q_v that roughly follow Clausius–Clapeyron scaling, while NorESM1-M's decreases in
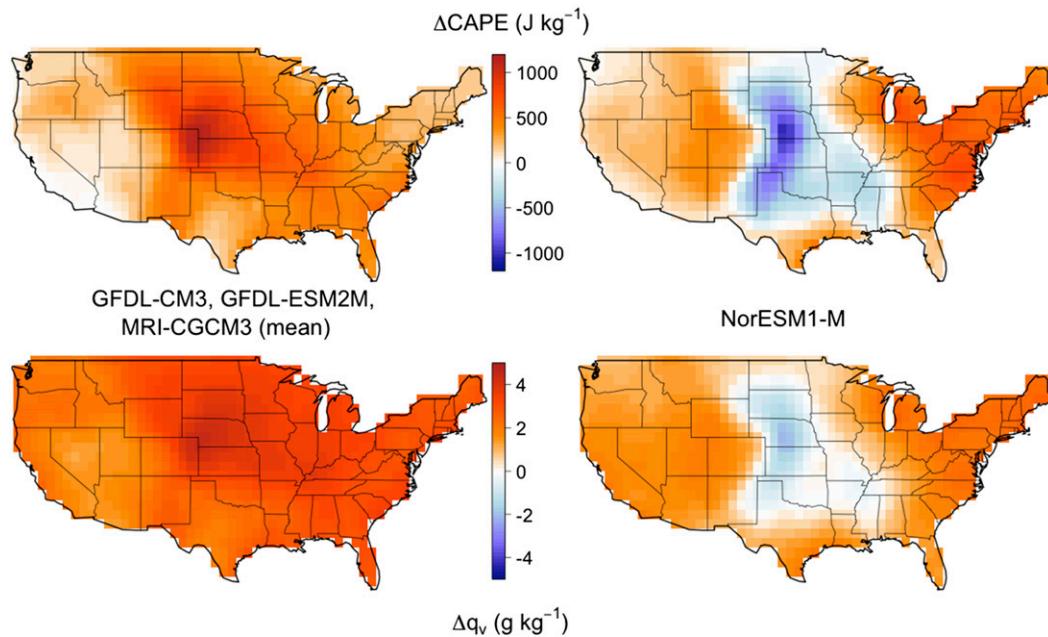
FIG. 7. Changes in JJA (top) CAPE and (bottom) boundary layer q_v in (left) the high-performing GFDL CM3, GFDL-ESM2M, and MRI-CGCM3 (mean of these three models) and (right) NorESM1-M. Changes are calculated as the mean of the period 1996–2005 of the CMIP5 historical experiment subtracted from the mean of the period 2079–88 of the RCP8.5 experiment.

CAPE are driven by a widespread aridification of the Great Plains. A time series of NorESM1-M's boundary layer humidity throughout the twenty-first century (not shown) indicates that our chosen time period is not simply anomalously dry for this model—the drying trend emerges around the year 2050 and persists thereafter. Such a drying out in the twenty-first century, while being opposite the observed twentieth-century trend (Dai 2006), is not impossible.

In any case, the results of Figs. 5 and 7 show that simulated future changes in thunderstorm severity are closely tied to changes in boundary layer humidity, as has been argued previously (T07; Trapp et al. 2009; D13). This suggests that focusing model development on the processes responsible for low-level humidification—from the influence of soil moisture to advection from the Gulf of Mexico into the Great Plains—is an important step toward further constraining the severe thunderstorms–global warming connection.

b. Sensitivity to γ

In the analysis presented thus far, STEnvs were identified for radiosonde and GCM data when Eq. (1) with $\gamma = 1$ and $\beta = 36\,300\,(\mathrm{m\,s}^{-1})^3$ was satisfied. These choices of parameters give equal weight to the value of CAPE and the value of shear, and select the upper 3% of the product of (CAPE)(shear) at 0000 UTC in the decade of radiosonde data spanning 1999–2008. However, multiple

studies have argued that the value of ambient wind shear has more influence on a given thunderstorm's severity than the local CAPE environment, suggesting that Eq. (1) with a value of γ closer to 1.6 or 1.7 is better at identifying environments favorable for severe thunderstorms (Brooks et al. 2003; Allen et al. 2011; Brooks 2013). In this section, we test the sensitivity of the results presented in section 3a to the choice of γ by repeating our analysis of CONUS-mean fractional changes in STEnvs while allowing γ to range from 1 to 2.

As γ is varied, the threshold β is varied as well to keep constant the number of STEnvs occurring for the radiosonde data. [That is, β is adjusted to select the upper 3% of (CAPE)(shear)$^\gamma$ in the decade of observations, regardless of γ. This reflects the fact that the number of severe thunderstorms that actually occurs does not depend on the details of an empirical threshold.] Varying β and γ in this way does not qualitatively affect the observational climatology of STEnvs (the annual climatologies are correlated with one another with an R^2 in the range of 0.99–0.85 over the range of γ), nor does it significantly affect the separation of models into the high- and low-performing groups presented in section 2. Table 2 gives the threshold β used for each value of γ in this analysis.

The sensitivity to γ of the changes in CONUS-mean STEnvs predicted by the high-performing models is shown in Fig. 8. Given that the effect of climate change

TABLE 2. The value for β in Eq. (1), for each value of γ used to test the sensitivity of modeled changes in STEnvs. To always select the top 3% of (CAPE)(shear)$^\gamma$ in the decade 1999–2008 of radiosonde data, β is varied.

γ	β [$(\mathrm{m\,s}^{-1})^{2+\gamma}$]
1.0	36 300
1.1	48 630
1.2	65 270
1.3	87 740
1.4	118 230
1.5	159 540
1.6	215 590
1.7	291 640
1.8	395 270
1.9	536 300
2.0	729 000

on severe thunderstorms has long been cast as a competition between increasing CAPE and decreasing shear, one expects increasing γ to generally suppress increases in STEnvs. The sensitivity varies across models, seasons, and RCP forcing pathways, but the negative slope of the lines in Fig. 8 confirms this prediction. MRI-CGCM3 is the most sensitive to changes in γ for all seasons and forcing pathways, with its summertime increases in RCP8.5 STEnvs reduced from roughly 60% to 30%. Similarly, the small decreases predicted by NorESM1-M in the summer when forced by RCP8.5 emissions become more negative when γ is increased from 1 to 2.

Overall, the relatively gentle slopes of the sensitivity lines in Fig. 8, even up to values of γ that exceed what has been suggested before by Brooks (2013) and others, imply that the qualitative results of GCM experiments when using $\gamma = 1$ will not differ substantially from those for $\gamma = 1.6$–1.7. Given the many other sources of unpredictability inherent to modeling future large-scale convective environments, Fig. 8 suggests that the relative weight given to shear and CAPE in the definition of a severe-thunderstorm-favorable environment is not the dominant source of uncertainty in this line of research. This builds confidence in the picture of future severe-thunderstorm increases given by our Figs. 4 and 5 and puts previous work by D13 and others who used $\gamma = 1$ to predict increases in United States severe-thunderstorm environments on more solid ground.

4. Conclusions

This study was motivated by two significant holes in our current understanding of the influence of global warming on severe thunderstorms in the United States. First, the analysis of D13 did not find statistically robust changes for summertime severe-thunderstorm environments in their 10-member ensemble of CMIP5 climate models. To

test if some of the divergence in their ensemble's predictions for the future could be traced to differences between models in their simulation of severe-thunderstorm conditions in the current climate, we looked at changes in STEnvs in a subset of four CMIP5 GCMs that were best able to match a radiosonde climatology of STEnvs. Our Fig. 5 shows that—even when focusing on high-performing models—there is disagreement on the sign of domain-mean summertime changes in future severe-thunderstorm environments under RCP8.5 forcing. For the months of June, July, and August, the outlier in the high-performing group of models is NorESM1-M, which, unlike GFDL CM3, GFDL-ESM2M, and MRI-CGCM3, predicts a widespread aridification of the central United States and a corresponding decrease in convective instability in the twenty-first century. This suggests that purely from the perspective of storm ingredients (i.e., neglecting changes in initiation), the future severity of thunderstorms is closely tied to low-level humidification. As such, further study of low-level humidification processes seems to be a prerequisite for achieving some level of consensus among climate models about future changes in summertime severe thunderstorms.

The second nagging source of uncertainty in projections of future thunderstorm severity addressed by this work is the fact that previous climate model studies of United States storms have all given equal weight to CAPE and wind shear in determining how "favorable" an environment is for severe thunderstorms (T07; Trapp et al. 2009; D13; Gensini et al. 2014), despite the fact that observational studies have argued that shear is more important than CAPE in determining a given thunderstorm's severity (Brooks et al. 2003; Allen et al. 2011; Brooks 2013). The results of our Fig. 8 suggest that the relative weight given to shear is not the dominant source of uncertainty in projections of future thunderstorm severity (i.e., each model's changes due to a unit increase in γ are smaller than the intermodel spread, even among just the high-performing models). This increases the level of confidence one may have in our results and those of previous work by D13 and others.

Overall, this study adds to the growing consensus that there will be more annual severe-thunderstorm-favorable combinations of CAPE and wind shear in a warm future United States, but there remain many unanswered questions about the future of severe thunderstorms. A largely unexplored subtlety in the use of CAPE–shear discriminant lines is the fact that not all storm environments above the discriminant line have equal probability of giving rise to severe thunderstorms, with environments farther above the line more likely to do so than those just barely exceeding the threshold. It should be possible to glean some useful information from the mean "distance"
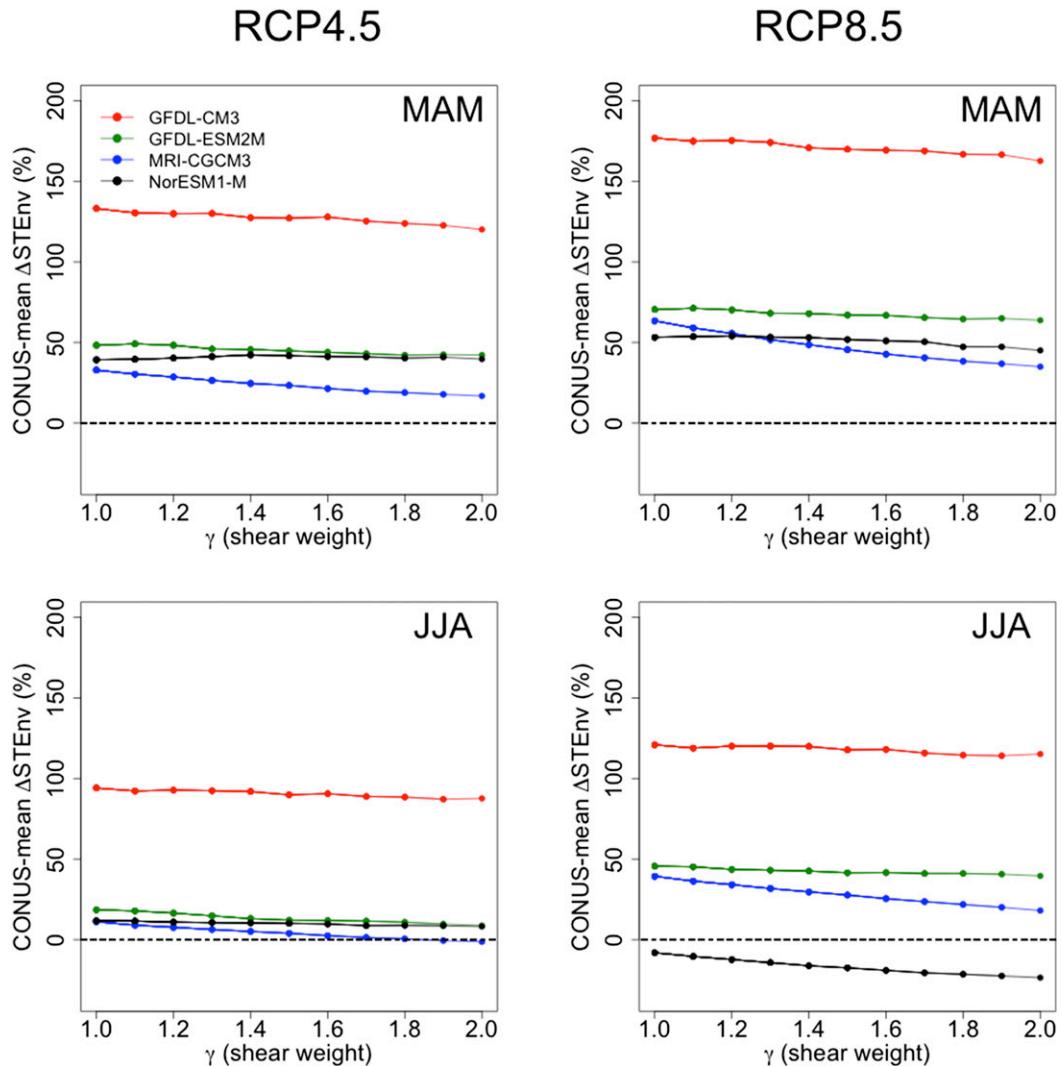
FIG. 8. The dependence of global-warming-induced CONUS-mean percent changes in STEnvs on the value of γ in Eq. (1), which defines the relative weight given to shear with respect to CAPE in determining whether a large-scale environment is considered favorable for severe thunderstorms. Results for the RCP4.5 and RCP8.5 emissions pathways and both MAM and JJA are shown. The slope of the line for each model gives an estimate of the sensitivity of that model's CONUS-mean percent changes in STEnvs to a unit increase in γ from 1 to 2.

of storm-favorable environments above any given discriminant line and refine the picture that results from only considering changes in the frequency of threshold exceedance.

The chief remaining source of uncertainty is the fact that, out of necessity, we have had to assume that the fraction of severe-thunderstorm environments developing into actual storms will be constant in time. This assumption is not well justified, and future changes in convective inhibition, extratropical storm tracks, and other processes known to be intimately related to storm initiation would have amplifying or attenuating effects on the trends in STEnvs identified here. These subjects

will be ripe for investigation as GCM resolutions continue to improve in coming years.

FIG. A1. The locations of the 68 SPARC radiosonde stations in CONUS.

APPENDIX

Data and Methods

Calculation of CAPE and shear

In this work, we diagnose convective instability using convective available potential energy (CAPE), which is the vertically integrated Archimedean buoyancy of a parcel of air taken from near the surface and lifted adiabatically through a column of the atmosphere. The precise value of CAPE associated to a column of the atmosphere depends on many assumptions about the definition of a parcel, the role of entrainment, and the treatment of fusion and condensate loading. These varying conventions have quantitative, not qualitative, effects on climatological CAPE values, and no one form of CAPE has been shown to be best suited to diagnosing severe-thunderstorm environments. In this work we choose to use nondilute, near-surface-based, adiabatic CAPE defined as follows:

$$\text{CAPE} = \max_p \int_p^{p_s} \left(\frac{1}{\rho_p} - \frac{1}{\rho_e} \right) dp', \qquad \text{(A1)}$$

where ρ_e is the environmental air density and ρ_p the parcel density. In practice, the above integral was trapezoidally approximated by calculating the buoyancy of a near-surface parcel at a series of discrete pressure levels in the radiosonde or GCM data. Parcel densities were calculated by using a root solver to find the thermodynamic state consistent with the equivalent potential temperature of the near-surface air. For this purpose, we use an exact expression for equivalent potential temperature derived by Romps and Kuang (2010), which includes the effects of latent heat of fusion and the different heat capacities of the water phases.

A number of measures of vertical wind shear have been used in combination with some criterion of instability to discriminate between severe and nonsevere convective environments (Craven and Brooks 2004). The two previous multimodel studies of severe-thunderstorm forcing

in the United States have used the magnitude of the difference between the horizontal wind vector near the surface and 6 km above the surface (T07; D13), and we do the same here, with one small difference: we take the upper-level winds from the pressure level equal to the mean of the surface pressure and 100 mbar. This ensures that the upper-level height adjusts upward with topography; with this definition, the mean height of over the CONUS is about 6 km. This has very minor effects on the sounding-by-sounding and climatological wind shear values.

Calculating these metrics of storm potential for a GCM column results in one value of CAPE and one value of shear associated with an area that is ~100–200 km on a side, whereas when calculating from a radiosonde one obtains values associated to a particular weather station within a network of such stations spread hundreds of kilometers apart (Fig. A1). To allow for comparison between the radiosonde network data and GCMs with varying resolutions, we bicubically interpolate all CAPE and shear values to a uniform 1° grid over the contiguous United States. The bicubic interpolation method was chosen for its speed, and negative values of CAPE that are generated by this interpolation are set to zero.

1) RADIOSONDE DATA

To produce a benchmark climatology of CAPE that is untainted by the parameterization of convection in reanalysis models, one must appeal directly to radiosonde data. For this work, we use the Stratosphere–Troposphere Processes and their Role in Climate (SPARC) high-vertical-resolution radiosonde data (HVRRD) record, which includes daily radiosonde releases at 0000 and 1200 UTC from 68 stations spread across the contiguous United States (Fig. A1) during the years 1999–2008 (World Climate Research Programme 2014). We use only the 0000 UTC radiosonde releases (from local mid- to late afternoon) and disregard the 1200 UTC radiosondes, which are released during local nighttime. Common-sense

filtering was applied to every sounding to exclude faulty data; a sounding was marked as "missing" due to any of the following indications of instrument malfunction or processing error:

- Malformed or corrupted data file
- Any pressure or elevation value missing
- Any air temperature value missing or outside the range of 100–400 K
- Pressure values increasing with time below 100 mbar
- Elevation values decreasing with time below 100 mbar
- Lapse rate greater than $50\,K\,km^{-1}$ for a 6-s interval at an elevation below 5 km
- Change in relative humidity between the first and second reports greater than 20%
- Wind speed greater than $100\,m\,s^{-1}$

After filtering, each legitimate sounding was interpolated to a uniform 100-m vertical resolution.

2) CLIMATE MODEL DATA

In this work, we use output from global climate models archived in phase 5 of the Coupled Model Intercomparison Project (CMIP5; Taylor et al. 2012). CMIP5 collects data from modeling groups from around the world who run a common set of experiments with the same initial conditions and forcings. At the time of writing, subdaily 3D fields of the variables required for calculating CAPE and shear at 0000 UTC are available for 11 global climate models in the CMIP5 archive. We summarize the institutional affiliations and spatial resolution of the GCMs used in this work in Table 1.

To evaluate the ability of the GCMs in our ensemble to simulate severe-thunderstorm activity in the current climate, we use data from the "historical" experiments. We take our control period to be the decade 1996–2005. This choice of decade of GCM data is dictated by the desire to match the decade covered by the radiosonde data (1999–2008) as closely as possible; since the historical experiments cover the period 1850–2005 before serving as the launch point for the future climate experiments (which run from 2006 through the end of the twenty-first century), the decade 1996–2005 is the closest match that does not begin to include the divergent forcing scenarios that are used for the future climate experiments. For future projections, we use the decade 2079–88 from the RCP4.5 and RCP8.5 scenarios, which correspond to increases in global radiative forcing of ~4.5 and ~8.5 $W\,m^{-2}$ over preindustrial levels by the late twenty-first century, respectively (van Vuuren et al. 2011). This choice of decade is dictated by data availability, as some of the models in our ensemble have not submitted data to CMIP5 that extends to the year 2100.

REFERENCES

Allen, J. T., D. J. Karoly, and G. A. Mills, 2011: A severe thunderstorm climatology for Australia and associated thunderstorm environments. *Aust. Meteor. Oceanogr. J.,* **61,** 143–158.

——, ——, and K. Walsh, 2014a: Future Australian severe thunderstorm environments. Part I: A novel evaluation and climatology of convective parameters from two climate models for the late twentieth century. *J. Climate,* **27,** 3827–3847, doi:10.1175/JCLI-D-13-00425.1.

——, ——, and ——, 2014b: Future Australian severe thunderstorm environments. Part II: The influence of a strongly warming climate on convective environments. *J. Climate,* **27,** 3848–3868, doi:10.1175/JCLI-D-13-00426.1.

Brooks, H. E., 2013: Severe thunderstorms and climate change. *Atmos. Res.,* **123,** 129–138, doi:10.1016/j.atmosres.2012.04.002.

——, and C. A. Doswell, 2001: Some aspects of the international climatology of tornadoes by damage classification. *Atmos. Res.,* **56,** 191–201, doi:10.1016/S0169-8095(00)00098-3.

——, and N. Dotzek, 2008: The spatial distribution of severe convective storms and an analysis of their secular changes. *Climate Extremes and Society,* H. F. Diaz and R. J. Murnane, Eds., Cambridge University Press, 35–54.

——, C. A. Doswell, and J. Cooper, 1994: On the environments of tornadic and nontornadic mesocyclones. *Wea. Forecasting,* **9,** 606–618, doi:10.1175/1520-0434(1994)009<0606:OTEOTA>2.0.CO;2.

——, J. W. Lee, and J. P. Craven, 2003: The spatial distribution of severe thunderstorm and tornado environments from global reanalysis data. *Atmos. Res.,* **67–68,** 73–94, doi:10.1016/S0169-8095(03)00045-0.

Carlson, T. N., and F. H. Ludlam, 1968: Conditions for the occurrence of severe local storms. *Tellus,* **20,** 203–226, doi:10.1111/j.2153-3490.1968.tb00364.x.

Craven, J. P., and H. E. Brooks, 2004: Baseline climatology of sounding-derived parameters associated with deep moist convection. *Natl. Wea. Dig.,* **28,** 13–24.

Dai, A., 2006: Recent climatology, variability, and trends in global surface humidity. *J. Climate,* **19,** 3589–3606, doi:10.1175/JCLI3816.1.

Diffenbaugh, N. S., R. J. Trapp, and H. E. Brooks, 2008: Does global warming influence tornado activity? *Eos, Trans. Amer. Geophys. Union,* **89,** 553–554, doi:10.1029/2008EO530001.

——, M. Scherer, and R. J. Trapp, 2013: Robust increases in severe thunderstorm environments in response to greenhouse forcing. *Proc. Natl. Acad. Sci. USA,* **110,** 16361–16366, doi:10.1073/pnas.1307758110.

Doswell, C. A., H. E. Brooks, and M. P. Kay, 2005: Climatological estimates of daily local nontornadic severe thunderstorm probability for the United States. *Wea. Forecasting,* **20,** 577–595, doi:10.1175/WAF866.1.

Field, C. B., Ed., 2012: *Managing the Risks of Extreme Events and Disasters to Advance Climate Change Adaptation.* Cambridge University Press, 582 pp.

Fritsch, J. M., R. J. Kane, and C. R. Chelius, 1986: The contribution of mesoscale convective weather systems to the warm-season precipitation in the United States. *J. Climate Appl. Meteor.,* **25,** 1333–1345, doi:10.1175/1520-0450(1986)025<1333:TCOMCW>2.0.CO;2.

Gensini, V. A., and W. S. Ashley, 2011: Climatology of potentially severe convective environments from North American Regional Reanalysis. *Electron. J. Severe Storms Meteor.,* **6** (8). [Available online at http://www.ejssm.org/ojs/index.php/ejssm/article/viewArticle/85.]

——, C. Ramseyer, and T. L. Mote, 2014: Future convective environments using NARCCAP. *Int. J. Climatol.,* **34,** 1699–1705, doi:10.1002/joc.3769.

Johns, R. H., and C. A. Doswell, 1992: Severe local storms forecasting. *Wea. Forecasting,* **7,** 588–612, doi:10.1175/1520-0434(1992)007<0588:SLSF>2.0.CO;2.

Kelly, D. L., J. T. Schaefer, and C. A. Doswell, 1985: Climatology of nontornadic severe thunderstorm events in the United States. *Mon. Wea. Rev.,* **113,** 1997–2014, doi:10.1175/1520-0493(1985)113<1997:CONSTE>2.0.CO;2.

Kunkel, K., and Coauthors, 2013: Monitoring and understanding trends in extreme storms: State of knowledge. *Bull. Amer. Meteor. Soc.,* **94,** 499–514, doi:10.1175/BAMS-D-11-00262.1.

Marsh, P. T., H. E. Brooks, and D. J. Karoly, 2007: Assessment of the severe weather environment in North America simulated by a global climate model. *Atmos. Sci. Lett.,* **8,** 100–106, doi:10.1002/asl.159.

National Weather Service, cited 2014: Severe weather definitions. [Available online at http://www.spc.noaa.gov/faq/.]

NOAA Storm Prediction Center, cited 2012a: Annual U.S. killer tornado statistics. [Available online at http://www.spc.noaa.gov/climo/torn/fataltorn.html.]

——, cited 2012b: Warning coordination meteorology. [Available online at http://www.spc.noaa.gov/wcm/.]

Rasmussen, E. N., 2003: Refined supercell and tornado forecast parameters. *Wea. Forecasting,* **18,** 530–535, doi:10.1175/1520-0434(2003)18<530:RSATFP>2.0.CO;2.

——, and D. O. Blanchard, 1998: A baseline climatology of sounding-derived supercell and tornado forecast parameters. *Wea. Forecasting,* **13,** 1148–1164, doi:10.1175/1520-0434(1998)013<1148:ABCOSD>2.0.CO;2.

Robinson, E. D., R. J. Trapp, and M. E. Baldwin, 2013: The geospatial and temporal distributions of severe thunderstorms from high-resolution dynamical downscaling. *J. Appl. Meteor. Climatol.,* **52,** 2147–2161, doi:10.1175/JAMC-D-12-0131.1.

Romps, D. M., 2011: Response of tropical precipitation to global warming. *J. Atmos. Sci.,* **68,** 123–138, doi:10.1175/2010JAS3542.1.

——, and Z. Kuang, 2010: Do undiluted convective plumes exist in the upper tropical troposphere? *J. Atmos. Sci.,* **67,** 468–484, doi:10.1175/2009JAS3184.1.

Singh, M., and P. O'Gorman, 2013: Influence of entrainment on the thermal stratification in simulations of radiative–convective equilibrium. *Geophys. Res. Lett.,* **40,** 4398–4403, doi:10.1002/grl.50796.

Sobel, A. H., and S. J. Camargo, 2011: Projected future seasonal changes in tropical summer climate. *J. Climate,* **24,** 473–487, doi:10.1175/2010JCLI3748.1.

Taylor, K. E., R. J. Stouffer, and G. A. Meehl, 2012: An overview of CMIP5 and the experiment design. *Bull. Amer. Meteor. Soc.,* **93,** 485–498, doi:10.1175/BAMS-D-11-00094.1.

Tebaldi, C., and R. Knutti, 2007: The use of the multi-model ensemble in probabilistic climate projections. *Philos. Trans. Roy. Soc.,* **365A,** 2053–2075, doi:10.1098/rsta.2007.2076.

Trapp, R. J., N. S. Diffenbaugh, H. E. Brooks, M. E. Baldwin, E. D. Robinson, and J. S. Pal, 2007a: Changes in severe thunderstorm environment frequency during the 21st century caused by anthropogenically enhanced global radiative forcing. *Proc. Natl. Acad. Sci. USA,* **104,** 19 719–19 723, doi:10.1073/pnas.0705494104.

——, B. A. Halvorson, and N. S. Diffenbaugh, 2007b: Telescoping, multi-model approaches to evaluate extreme convective weather under future climates. *J. Geophys. Res.,* **112,** D20109, doi:10.1029/2006JD008345.

——, N. S. Diffenbaugh, and A. Gluhovsky, 2009: Transient response of severe thunderstorm forcing to elevated greenhouse gas concentrations. *Geophys. Res. Lett.,* **36,** L01703, doi:10.1029/2008GL036203.

——, E. Robinson, M. Baldwin, N. Diffenbaugh, and B. Schwedler, 2011: Regional climate of hazardous convective weather through high-resolution dynamical downscaling. *Climate Dyn.,* **37,** 677–688, doi:10.1007/s00382-010-0826-y.

van Klooster, S., and P. Roebber, 2009: Surface-based convective potential in the contiguous United States in a business-as-usual future climate. *J. Climate,* **22,** 3317–3330, doi:10.1175/2009JCLI2697.1.

van Vuuren, D. P., and Coauthors, 2011: The representative concentration pathways: An overview. *Climatic Change,* **109,** 5–31, doi:10.1007/s10584-011-0148-z.

Verbout, S. M., H. E. Brooks, L. M. Leslie, and D. M. Schultz, 2006: Evolution of the U.S. tornado database: 1954–2003. *Wea. Forecasting,* **21,** 86–93, doi:10.1175/WAF910.1.

World Climate Research Programme, cited 2014: U.S. high vertical resolution radiosonde data. [Available online at http://www.sparc-climate.org/data-center/data-access/us-radiosonde/.]